Revealing conformational changes of GTP-bound NRAS mutants probed by GaMD and Markov state models

Lu Zhao [a,*], Jian Wang [a], Haipeng Ping [b], Wanchun Yang [a], Haijun Cao [a], Jianzhong Chen [a,*]

[a]School of Science, Shandong Jiaotong University, Jinan 250357, China.
[b]Smart City Evaluation and Assessment Center, Shandong Institute of Information Technology Industry Development, Jinan 250014, China.
Email: zhaolusdu@163.com, zhaolu@sdjtu.edu.cn, chenjianzhong1970@163.com, jzchen@sdjtu.edu.cn

Table S1 Atoms of the complexes and the systems.

Systems	**Atoms of the system**	**Atoms of protein-ligand complex**
GTP-bound WT NRAS	16657	2665
GTP-bound G12D NRAS	16663	2670
GTP-bound Q61R NRAS	16546	2672
GTP-bound C118S NRAS	16663	2665

Table S2 MFPTs for conformational transitions between the identified macrostates.

	MFPT(ns)	**State 1**	**State 2**	**State 3**	
GTP-bound	**State 1**	-	32.9	2.7	
WT NRAS	**State 2**	32	-	3.7	
	State 3	29.1	30.7	-	
	MFPT(ns)	**State 1**	**State 2**	**State 3**	**State 4**
GTP-bound	**State 1**	-	15	38.4	83
G12D NRAS	**State 2**	42	-	43	71.4
	State 3	105	69.6	-	14.5
	State 4	120.9	95.7	15.2	-
	MFPT(ns)	**State 1**	**State 2**	**State 3**	
GTP-bound	**State 1**	-	36.4	252.7	
Q61R NRAS	**State 2**	147.6	-	191.6	
	State 3	268	94.1	-	
	MFPT(ns)	**State 1**	**State 2**	**State 3**	**State 4**
GTP-bound	**State 1**	-	68.5	80.3	2.6
C118S NRAS	**State 2**	115.4	-	58.2	6.4
	State 3	128.4	60.8	-	18.4
	State 4	99.1	62.2	73.3	-

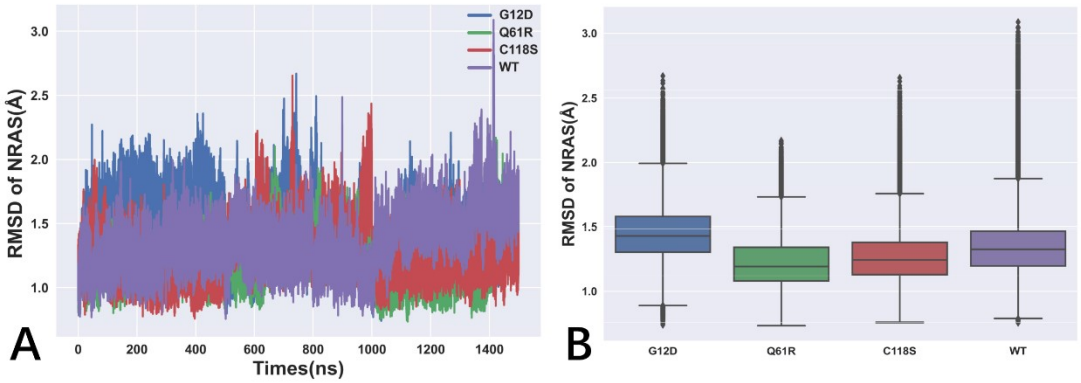

Fig. S1 RMSDs of heavy atoms from NRAS: (A) the time course of RMSDs for G12D, Q61R, C118S and WT NRAS, and (B) statistical distributions of RMSDs for G12D, Q61R, C118S and WT NRAS.

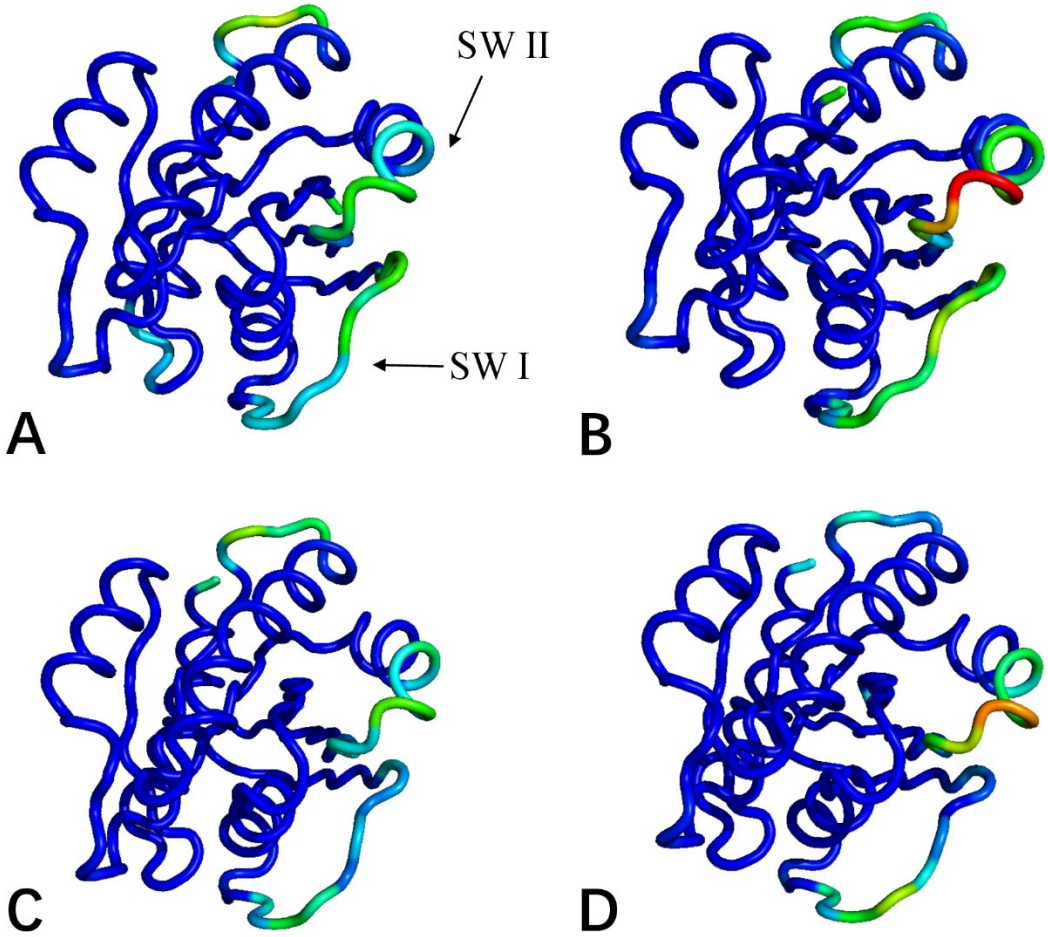

Fig. S2 B-factor representations of the NRAS structural flexibility: (A) WT NRAS, (B) G12D NRAS, (C) Q61R NRAS and (D) C118S NRAS. The tube representation of the NRAS structure is colored according to the B-factors, ranging from blue (low B-factor, indicating high rigidity) to red (high B-factor, indicating high flexibility).

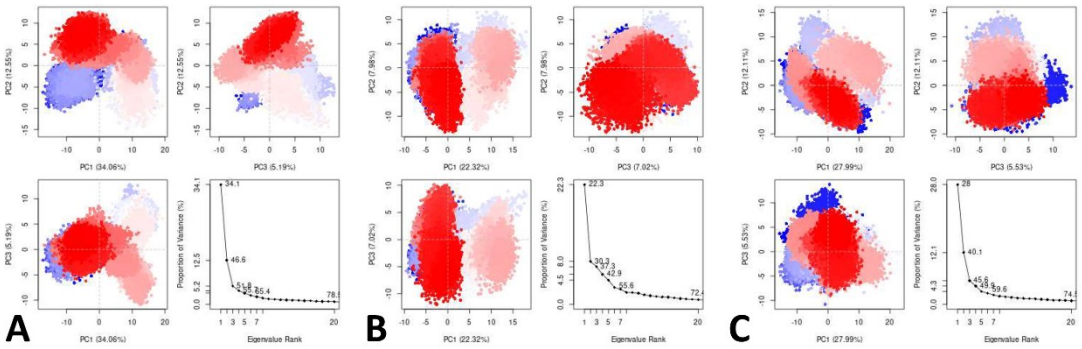

Fig. S3 Conformational transformations of GTP-bound NRAS revealed from the first three principal components (PC1−PC3): (A) GTP-bound G12D NRAS, (B) GTP-bound Q61R NRAS, and (C) GTP-bound C118S NRAS, in which the transformation from the red to the blue reflects the transitions between different conformation spaces of NRAS.

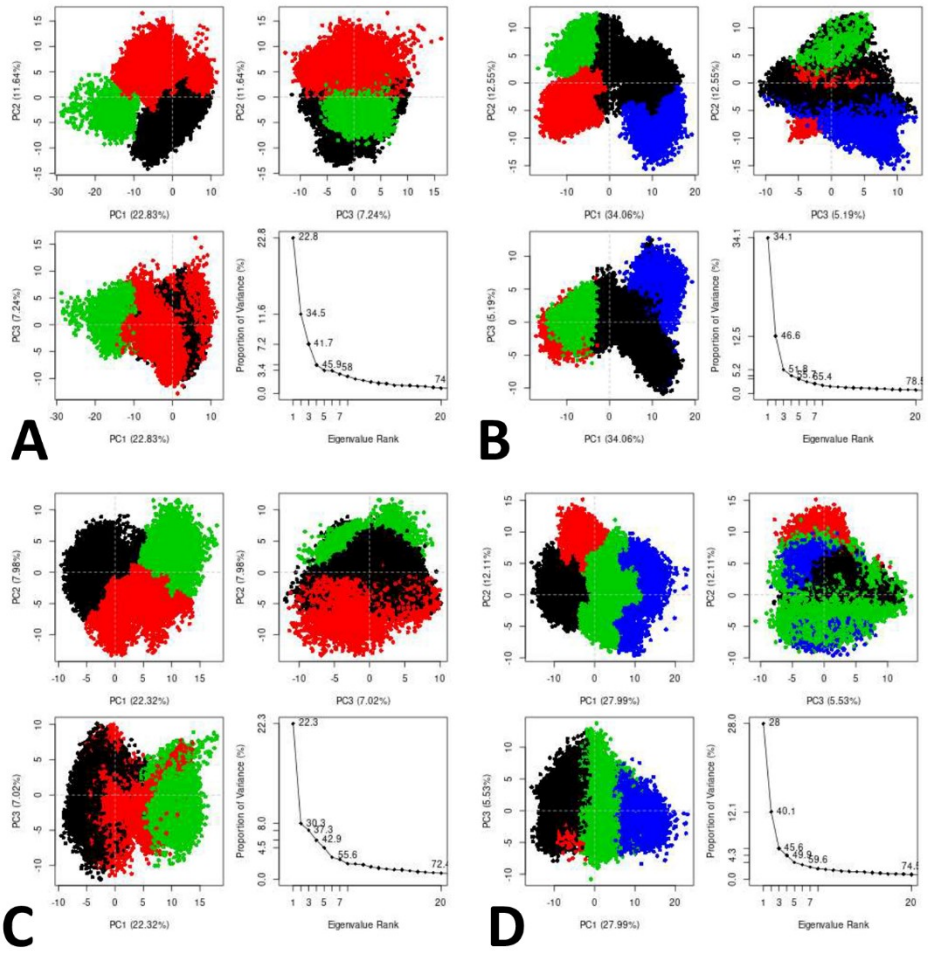

Fig. S4 Conformation clusters of NRAS by the PC1-PC3: (A) GTP-bound WT NRAS, (B) GTP-bound G12D NRAS, (C) GTP-bound Q61R NRAS, and (D) GTP-bound C118S NRAS.

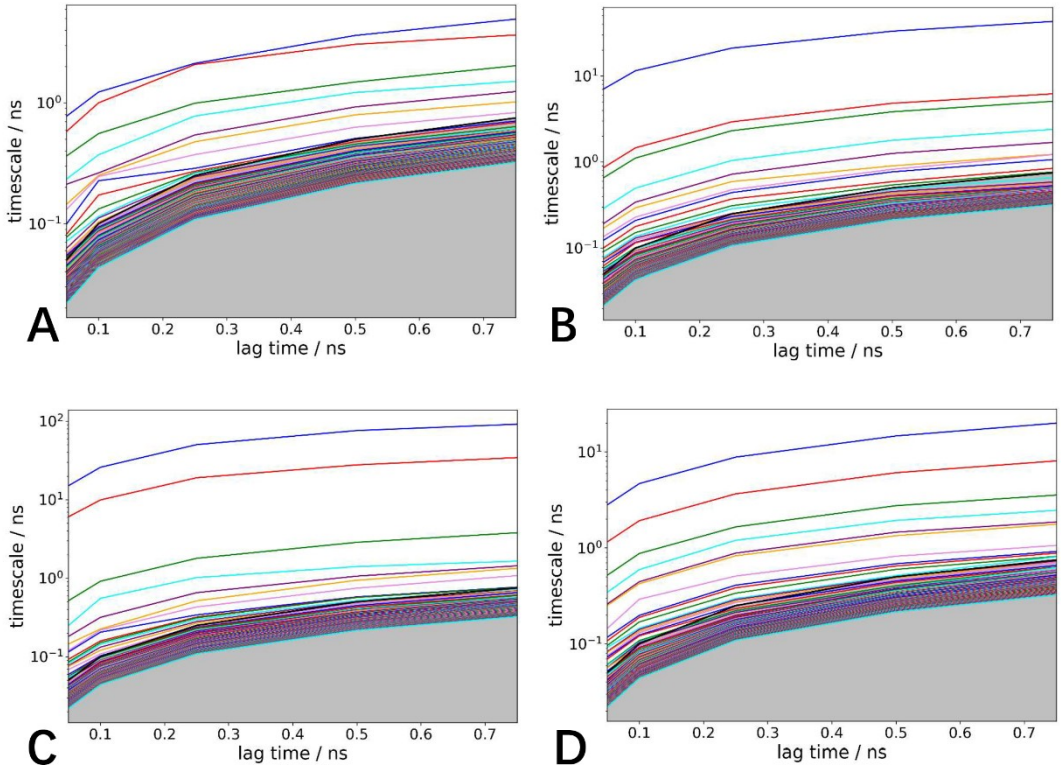

Fig. S5 Lag time determination of four systems: (A) GTP-bound WT NRAS, (B) GTP-bound G12D NRAS, (C) GTP-bound Q61R NRAS, and (D) GTP-bound C118S NRAS.

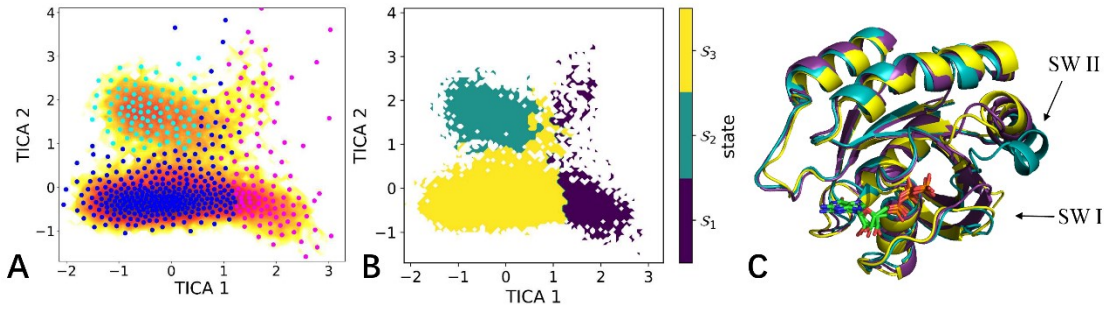

Fig. S6 Microstate distribution and macrostate representation of GTP-bound WT NRAS from MSM analysis: (A) distribution of the 500 microstates projected onto the first two TICA. Each microstate is colored according to its assignment to one of the three macrostates, (B) partitioning of the TICA space into three macrostates (S1, S2, and S3) in which each macrostate is represented by a distinct color: S1 (purple), S2 (teal), and S3 (yellow), and (C) superposition of the representative structures for each of the three macrostates (S1 in purple, S2 in teal, and S3 in yellow).

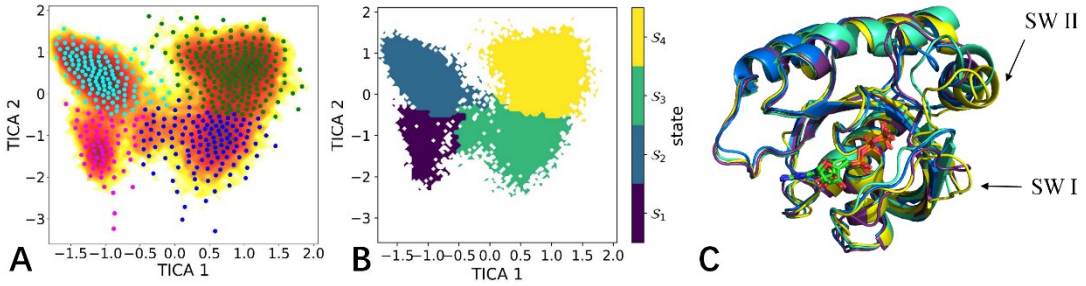

Fig. S7 Microstate distribution and macrostate representation of GTP-bound G12D NRAS from MSM analysis: (A) distribution of the 500 microstates projected onto the first two TICA, each microstate is colored according to its assignment to one of the four macrostates, (B) partitioning of the TICA space into four macrostates (S1, S2, S3 and S4) in which each macrostate is represented by a distinct color, namely S1 (purple), S2 (teal), S3 (green) and S4 (yellow), and (C) superposition of the representative structures for each of the four macrostates (S1 in purple, S2 in teal, S3 in green and S4 in yellow).

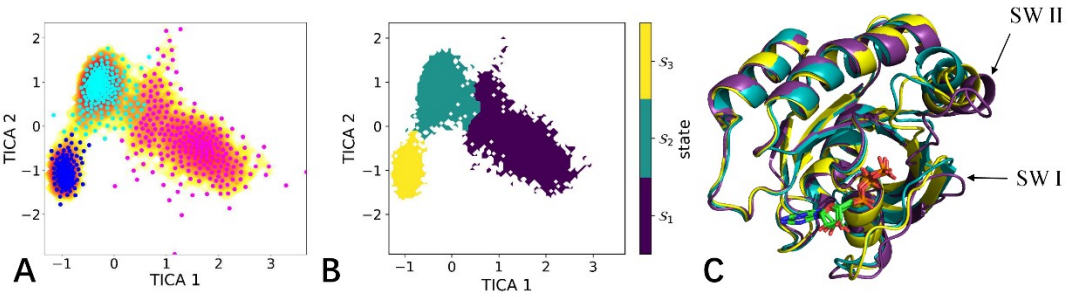

Fig. S8 Microstate distribution and macrostate representation of GTP-bound Q61R NRAS from MSM analysis: (A) distribution of the 500 microstates projected onto the first two TICA, in which each microstate is colored according to its assignment to one of the three macrostates, (B) partitioning of the TICA space into three macrostates (S1, S2, and S3), of which each macrostate is represented by a distinct color, namely S1 (purple), S2 (teal), and S3 (yellow), and (C) superposition of the representative structures for each of the three macrostates (S1 in purple, S2 in teal, and S3 in yellow).

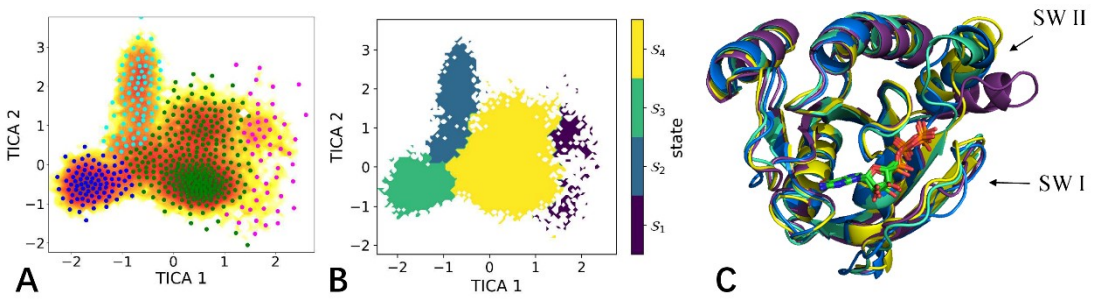

Fig. S9 Microstate distribution and macrostate representation of GTP-bound C118S NRAS from MSM analysis: (A) distribution of the 500 microstates projected onto the first two TICA, in which each microstate is colored according to its assignment to one of the four macrostates, (B) partitioning of the TICA space into four macrostates (S1, S2, S3 and S4), from which each macrostate is represented by a distinct color, involving S1 (purple), S2 (teal), S3 (green) and S4 (yellow), and (C) superposition of the representative structures for each of the four macrostates (S1 in purple, S2 in teal, S3 in green and S4 in yellow).

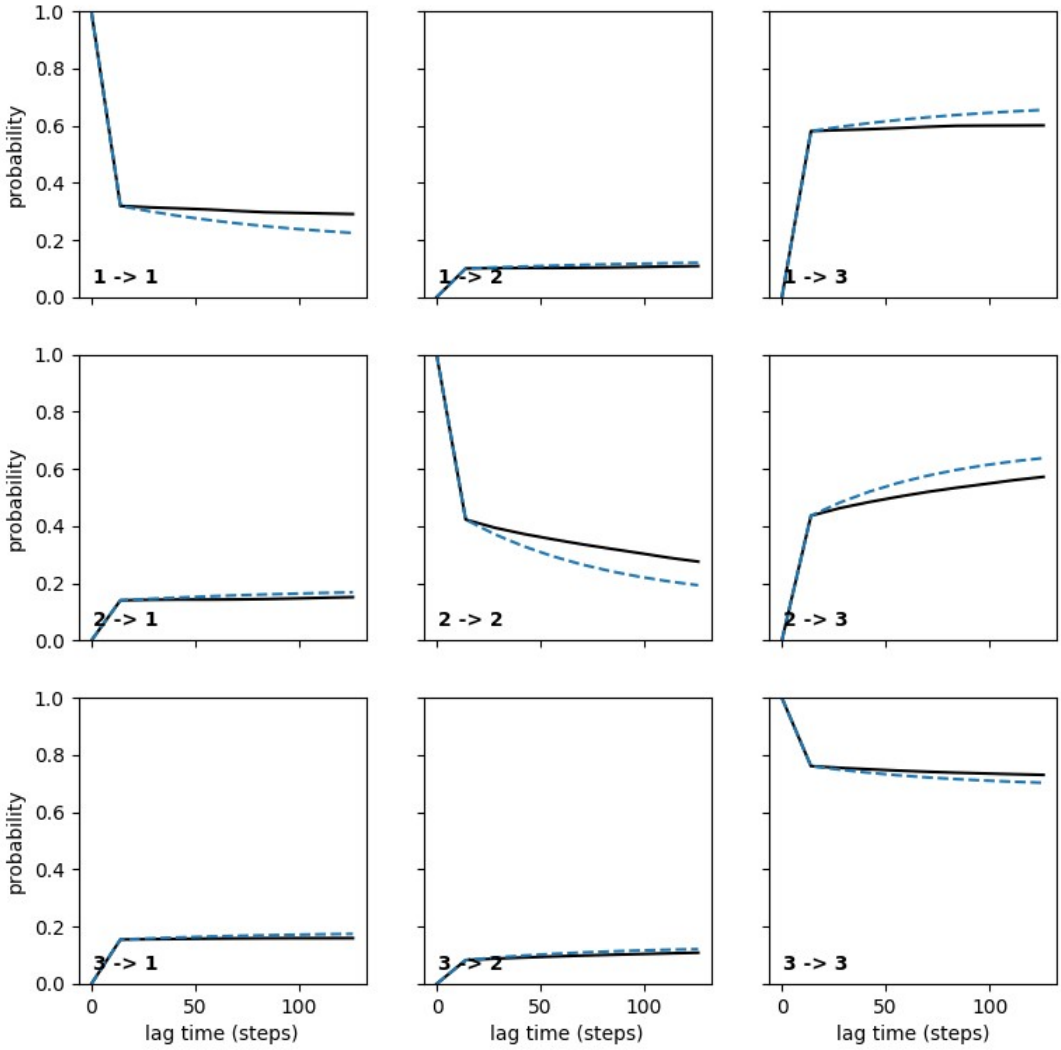

Fig. S10 Chapman-Kolmogorov (C-K) test applied to the Markov model of GTP-bound WT NRAS.

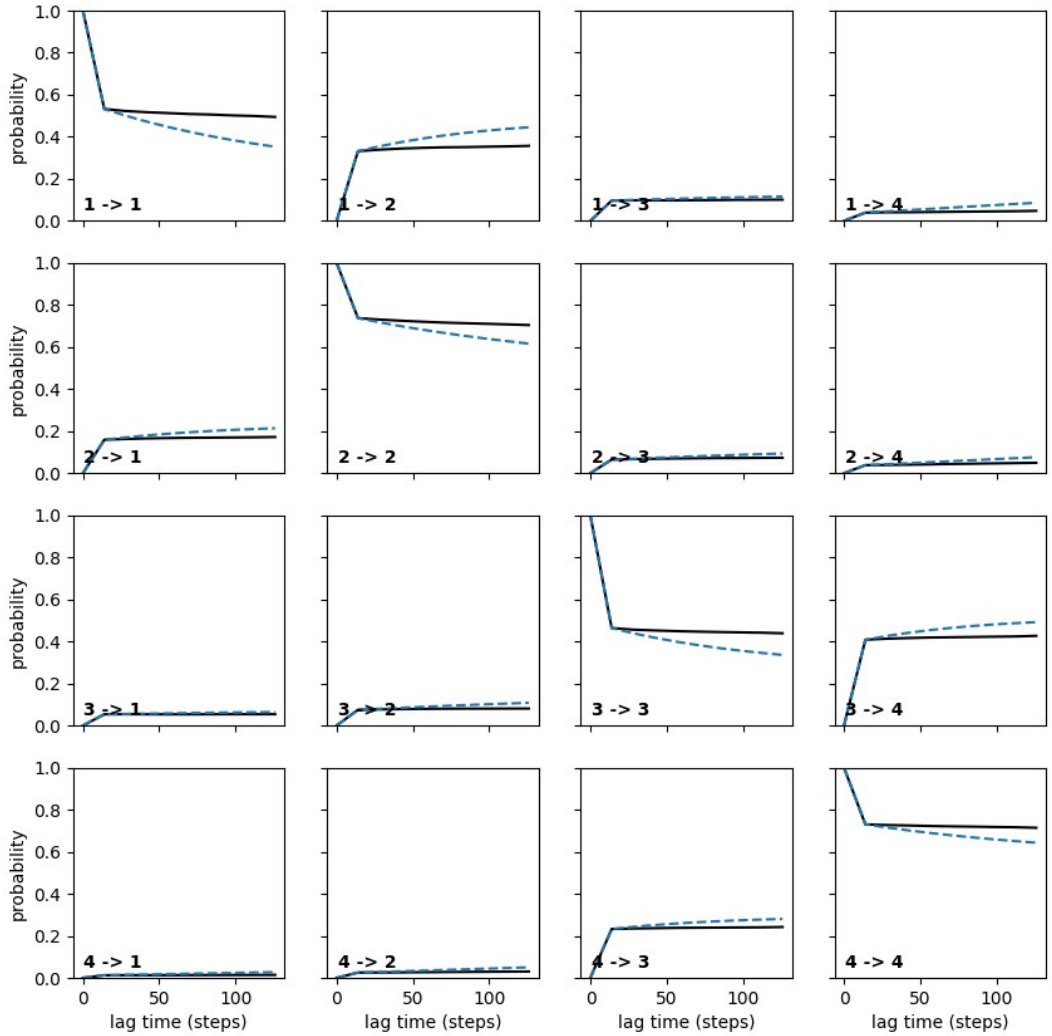

Fig. S11 Chapman-Kolmogorov (C-K) test applied to the Markov model of GTP-bound G12D NRAS.

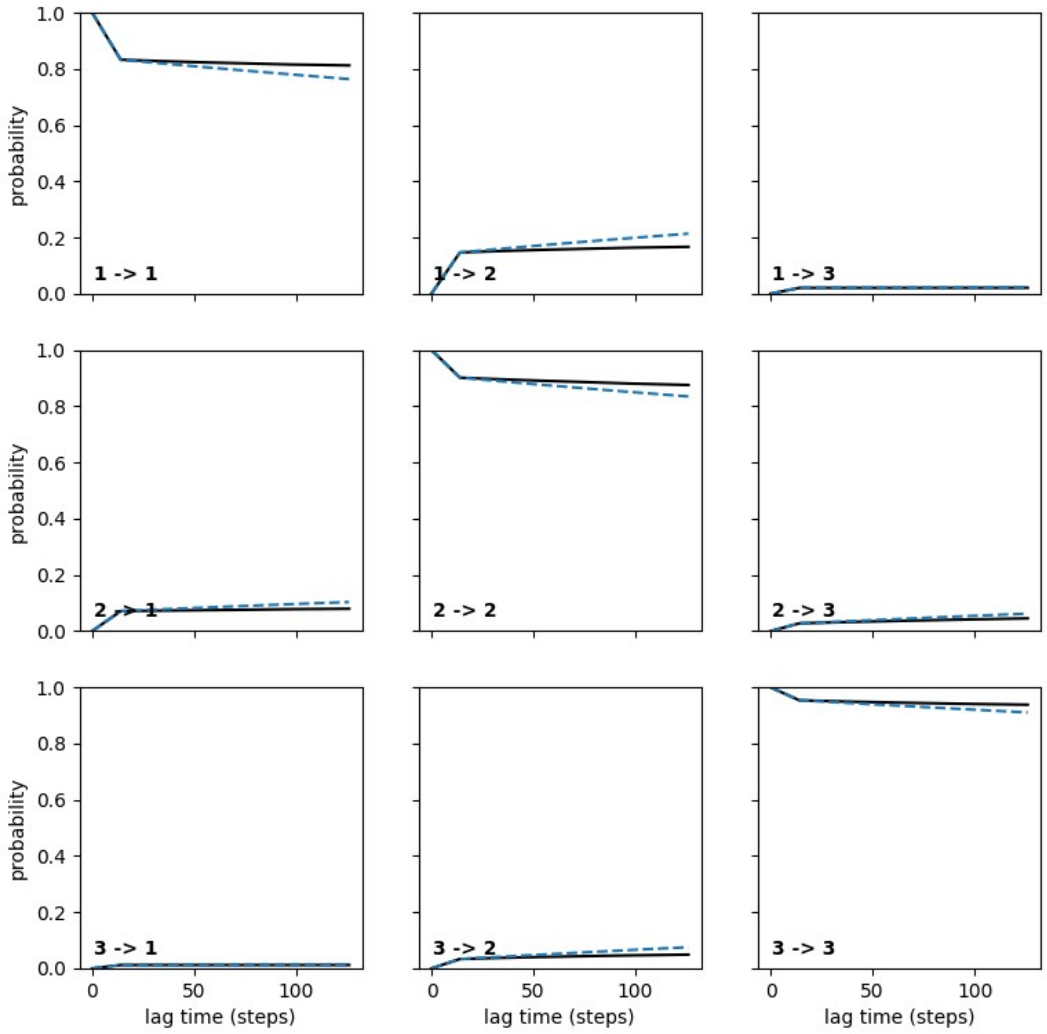

Fig. S12 Chapman-Kolmogorov (C-K) test applied to the Markov model of GTP-bound Q61R NRAS.

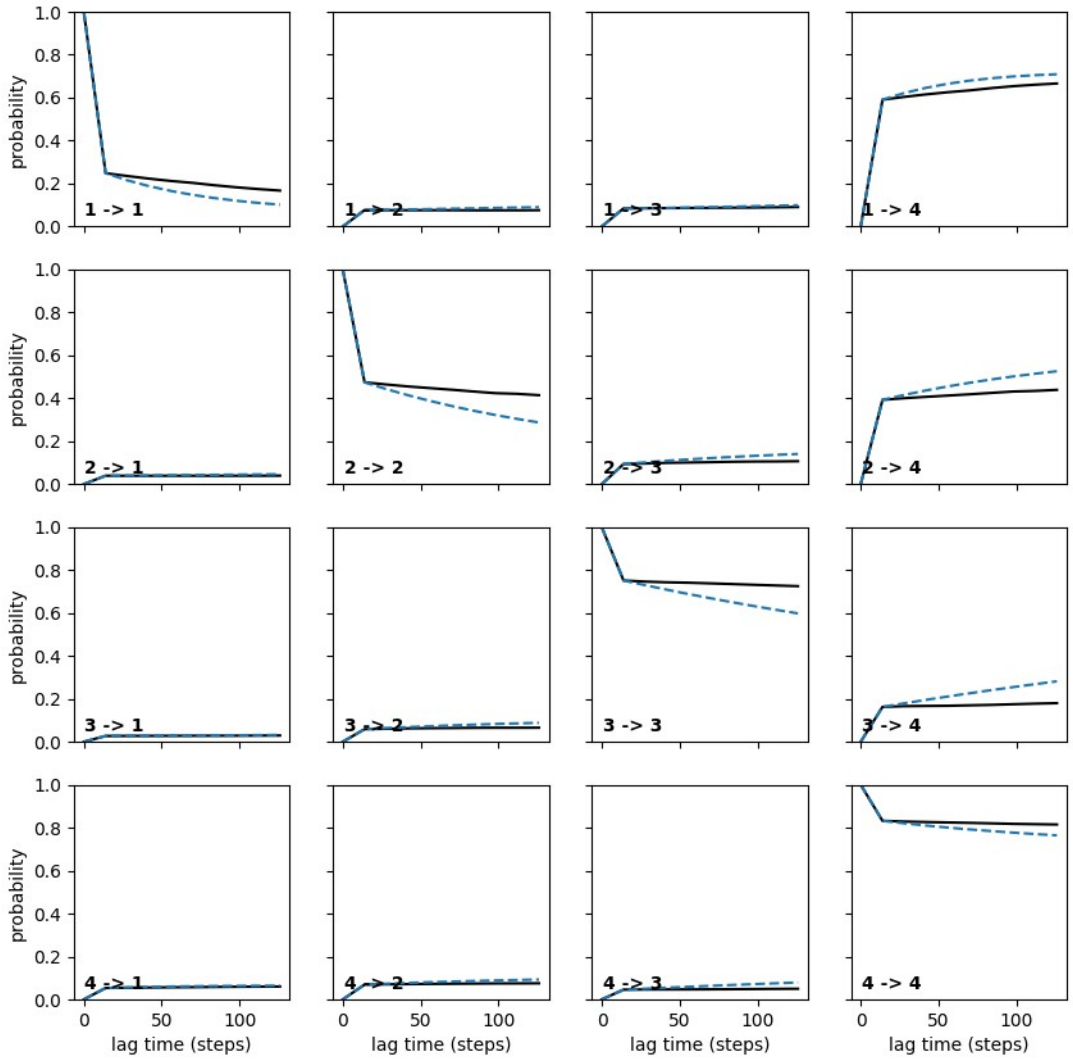

Fig. S13 Chapman-Kolmogorov (C-K) test applied to the Markov model of GTP-bound C118S NRAS.

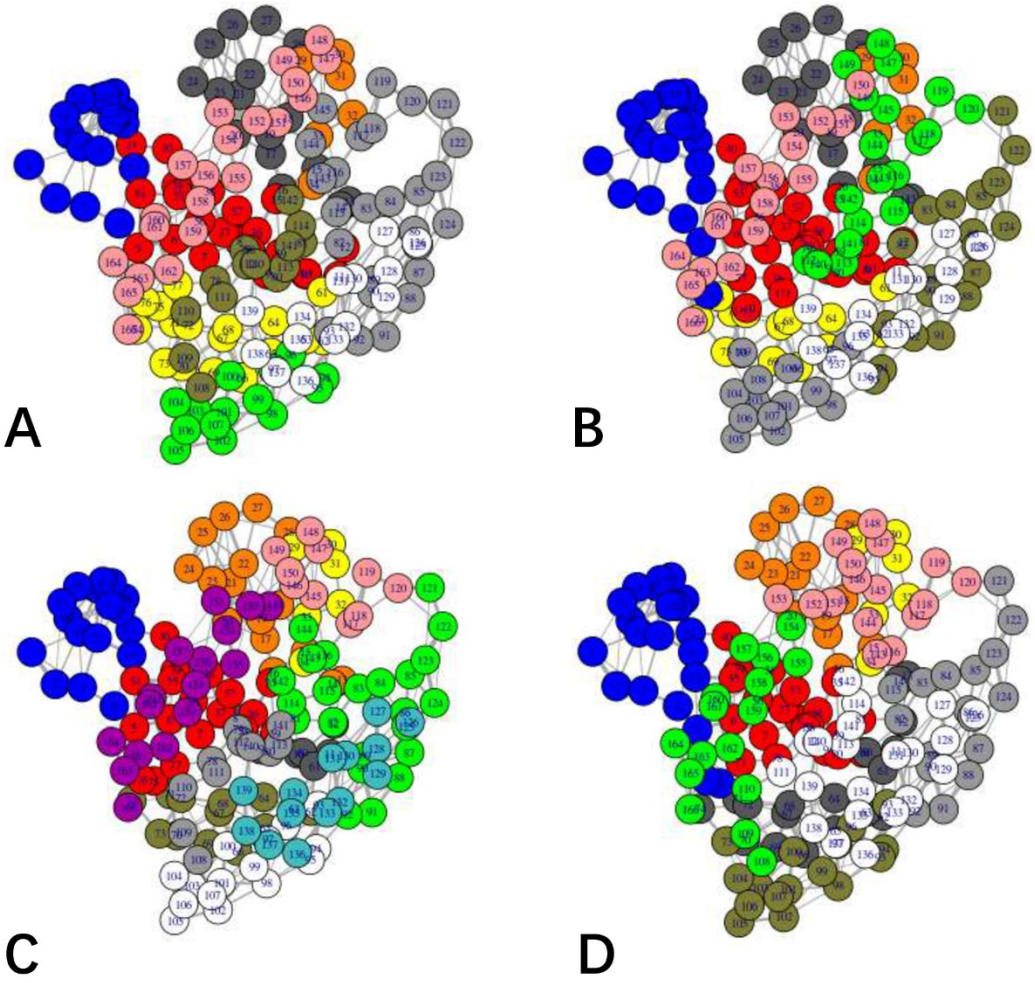

Fig. S14 Residue network communications between key structural domains of NRAS: (A) GTP-bound WT NRAS, (B) GTP-bound G12D NRAS, (C) GTP-bound Q61R NRAS, and (D) GTP-bound C118S NRAS.

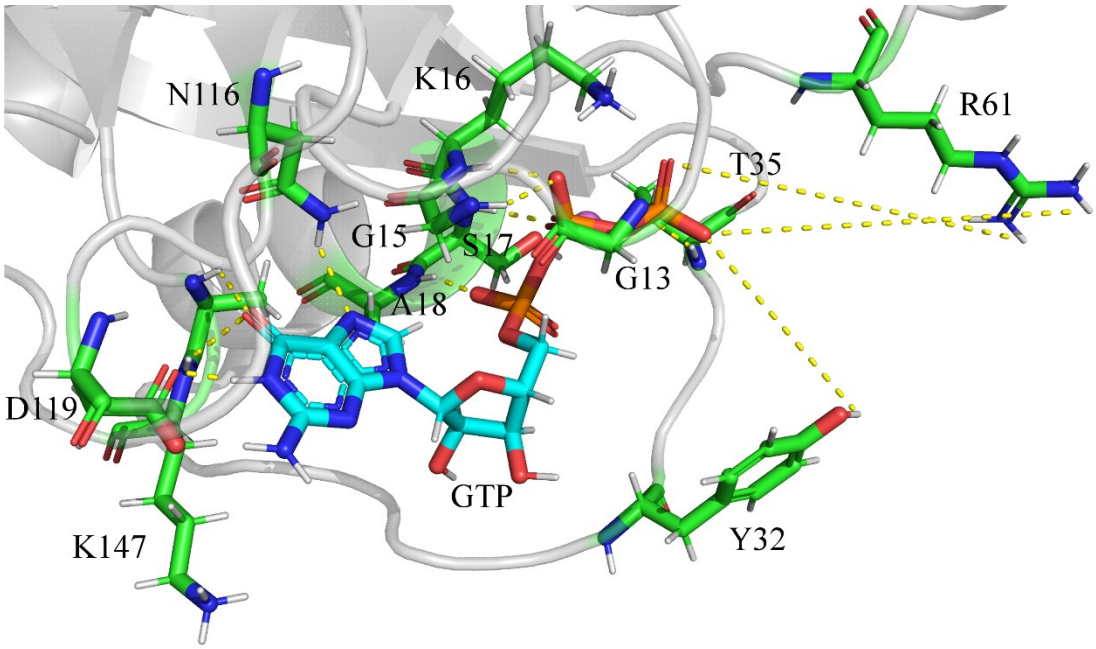

Fig. S15 Geometric position of key residues relative to GTP.

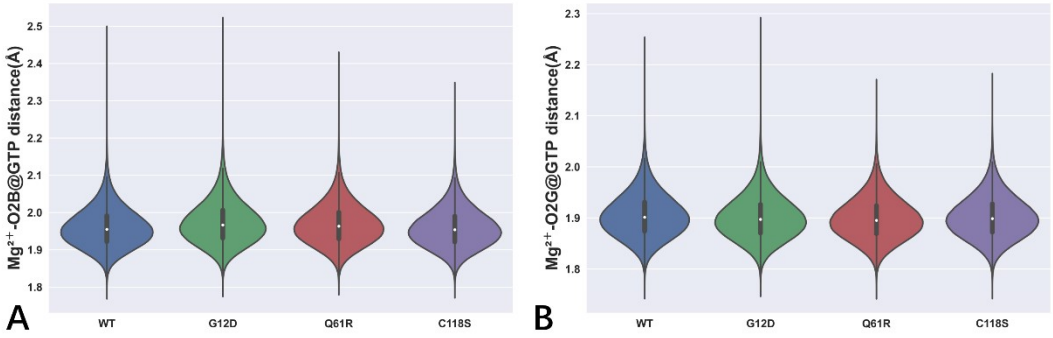

Fig. S16 Key interactions of magnesium ions (Mg^{2+}) with GTP together with their distance distributions: (A) the distances between Mg^{2+} and the oxygen atom O2B of GTP, and (B) the distances of Mg^{2+} away from the oxygen atom O2G of GTP.